NEOPLASIA
www.neoplasia.com

Volume 13 Number 3 March 2011 pp. 198–205 198

Cytoplasmic Overexpression of CD95L in Esophageal Adenocarcinoma Cells Overcomes Resistance to CD95-Mediated Apoptosis[1]

Gregory A. Watson, Sanjay Naran, Xinglu Zhang, Michael T. Stang, Pierre E. Queiroz de Oliveira and Steven J. Hughes

Department of Surgery, Division of Surgical Oncology, University of Pittsburgh, Pittsburgh, PA, USA

Abstract

INTRODUCTION: The CD95/CD95L pathway plays a critical role in tissue homeostasis and immune system regulation; however, the function of this pathway in malignancy remains poorly understood. We hypothesized that CD95L expression in esophageal adenocarcinoma confers advantages to the neoplasm other than immune privilege. *METHODS:* CD95L expression was characterized in immortalized squamous esophagus (HET-1A) and Barrett esophagus (BAR-T) cells; adenocarcinoma cell lines FLO-1, SEG-1, and BIC-1, and MDA468 (− control); and KFL cells (+ control). Analyses included reverse transcription–polymerase chain reaction, immunoblots of whole cell and secretory vesicle lysates, FACScan analysis, laser scanning confocal microscopy of native proteins and fluorescent constructs, and assessment of apoptosis and ERK1/2 pathways. *RESULTS:* Cleaved, soluble CD95L is expressed at both the RNA and protein levels in these cell lines derived from esophageal adenocarcinoma and other human tissues. CD95L was neither trafficked to the cell membrane nor secreted into the media or within vesicles, rather the protein seems to be sequestered in the cytoplasm. CD95 and CD95L colocalize by immunofluorescence, but an interaction was not proven by immunoprecipitation. Overexpression of CD95L in the adenocarcinoma cell lines induced robust apoptosis and, under conditions of pan-caspase inhibition, resulted in activation of ERK signaling. *CONCLUSIONS:* CD95L localization in EA cells is inconsistent with the conference of immune privilege and is more consistent with a function that promotes tumor growth through alternative CD95 signaling. Reduced cell surface expression of CD95 affects cell sensitivity to extracellular apoptotic signals more significantly than alterations in downstream modulators of apoptosis.

Neoplasia (2011) 13, 198–205

Introduction

The importance of alterations in apoptotic pathways to the development of malignancy is well established. CD95 (Fas/Apo-1) is a cell surface receptor and member of the "death receptor" family that includes the tumor necrosis factor receptors (TNFR1 and TNFR2), DR4 and DR5, and TRAIL [1,2]. Normally, CD95 transmits an apoptotic signal after binding by CD95 ligand (CD95L) [3]. Consistent with this function, near-universal resistance to CD95-mediated apoptosis has been observed in many malignancies [4]. However, loss of expression or inactivating mutation of CD95 is rarely observed in neoplasia [4]. In fact, activation of CD95 and other family members has been observed to stimulate p38, nuclear factor κB (NF-κB), and extracellular signal–regulated kinase 1/2 (ERK1/2) activities, and accumulating evidence suggests a potential role for CD95/CD95L pathway involvement in tumor development [5–7]. Very recently, Chen et al. [8] clearly demonstrated a role for CD95 in the promotion of tumor growth through a pathway involving the mitogen-activated protein kinases (MAP-k) JNK and Jun.

The CD95/CD95L system plays an essential role in T-cell development, and CD95L expression produces immune privilege in the placenta, testis, and the anterior chamber of the eye [9–11]. CD95L

Address all correspondence to: Steven J. Hughes, MD, 1600 SW Archer Rd, Room 6164, PO Box 100109, Gainesville, FL 32610-0109. E-mail: Steven.Hughes@surgery.ufl.edu
[1]This work was supported by National Institutes of Health grant CA-01958-05 (S.J.H.).
Received 9 September 2010; Revised 17 December 2010; Accepted 30 December 2010

DOI 10.1593/neo.101304

is also expressed by neoplastic tissues, and cancer patients frequently have elevated levels of CD95L [12–15]; however, acceptance of an immune privilege function of neoplastic CD95L expression remains controversial owing to conflicting experimental data [16,17]. Recent data have improved our understanding of the functions of membrane-bound CD95L (mCD95L) *versus* protease-cleaved soluble CD95L (sCD95L) showing that mCD95L only is essential for CD95-mediated apoptosis [18]. However, there remains a lack of adequate data regarding the expression and function of sCD95L *versus* mCD95L in neoplasia.

We have previously identified resistance to CD95-mediated apoptosis in esophageal adenocarcinoma (EA) and lung non–small cell cancer due to cytoplasmic retention of CD95 resulting in reduced cell surface expression [19,20]. Given the above background, we hypothesized that CD95 ligand expression in EA confers advantages other than immune privilege to the cell. The aims of this study were 1) to characterize posttranslational regulation and localization of CD95L expression in EA, 2) to determine whether cytoplasmic CD95-CD95L interactions occur in EA, and 3) to investigate the response of EA cells to activation of the cytoplasmic pool of CD95. We discovered that EA cells produce CD95L but relatively lack mCD95L expression, lack secretion of sCD95L, and provide data suggesting low levels of sCD95L expression in EA results in alternative MAP-k signaling. Most importantly, overexpression of CD95L within the cytoplasm of CD95-mediated apoptosis-resistant adenocarcinoma cells induces extensive apoptosis. This finding strongly suggests that posttranslational regulation of cell surface expression of death receptors affects cell sensitivity to extracellular apoptotic signals more significantly than alterations in downstream modulators of apoptotic pathways.

Materials and Methods

Cell Lines

All cell lines are human derived. The following cells were purchased from American Type Culture Collection (ATCC, Manassas, VA): Het-1A (squamous esophagus), Jurkat T cells (JTCs), and MDA468 (breast adenocarcinoma). The three adenocarcinoma cell lines (Seg-1, Bic-1, and Flo-1) have been previously described [19]. Since this earlier report, we have learned that only Flo-1 cells are of EA origin. DNA fingerprinting has demonstrated that Seg-1 cells are actually H460 lung adenocarcinoma cells, and Bic-1 cells are SW480 colon adenocarcinoma cells (D.G. Beer, personal communication). KFL (leukemia) [21] and BAR-T Barrett esophagus cells [22] were generous gifts from Drs David Kaplan and Rhonda Souza, respectively. Cell lines were maintained in RPMI-1640 (KFL, JTC, Het-1A, and Seg-1) or Dulbecco modified Eagle media (MDA468, Bic-1, and Flo-1) (BioWhittaker, Walkersville, MD) which were supplemented with 10% fetal bovine serum (Atlanta Biologicals, Norcross, GA), 1% penicillin/streptomycin, and 1% L-glutamine (Invitrogen, Carlsbad, CA). Barrett esophagus was maintained as previously described [22]. All cell lines were propagated in a humidified environment at 37°C with 5% CO_2.

Antibodies and Reagents

The following antibodies for immunoblot analysis were purchased from Santa Cruz Biotechnology, Inc (Santa Cruz, CA): constitutive heat shock protein 70 (Hsc70), ERK, and phospho-ERK. Other antibodies used for immunoblot analysis included caspase 8 and caspase 3 (Cell Signaling Technology, Inc, Beverly, MA), CD95 clone 5F-7 (Kamiya Biomedical Company, Seattle, WA), and β-actin (Sigma-Aldrich, Inc, St Louis, MO). Anti-CD95 clone CH11 (Upstate Biotechnology, Inc, Lake Placid, NY) was used for laser scanning confocal microscopy and apoptosis induction, and green fluorescent protein (GFP) and bovine serum albumin (BSA) antibodies (Abcam, Inc, Cambridge, MA) were used for immunoprecipitation. Anti-CD95L antibody clones NOK-1 and G247-4 (Becton Dickinson Pharmingen, San Diego, CA) were used for FACScan analysis of cell surface expression and immunoblot analysis/laser scanning confocal microscopy, respectively. All horseradish peroxidase– and fluorophor-conjugated secondary antibodies were purchased from Jackson Immunoresearch, Inc (West Grove, PA), and Draq5 was purchased from Biostatus, Ltd (Leicestershire, UK). The broad-spectrum matrix metalloproteinase (MMP) inhibitor GM-6001 and the pan-caspase inhibitor Z-VAD-FMK (zVad) were purchased from Chemicon International, Inc, (Temecula, CA) and Promega (Madison, WI), respectively.

CD95L and CD95 Reverse Transcription–Polymerase Chain Reaction

RNA was isolated from 90% confluent cultures using the RNEasy Mini Kit (Qiagen, Valencia, CA), and 2 μg of RNA was reverse-transcribed using the One Step RT-PCR Kit (Qiagen) according to the manufacturer's instructions. CD95L forward primer was 5′-GCCCTTCAATTACCCATATCCC-3′, and CD95L reverse primer was 5′-GGCAACCAGAACCATGAAAAACA-3′. Initial conditions for both reactions included a reverse transcription at 50°C for 30 minutes and a polymerase chain reaction (PCR) activation step at 95°C for 15 minutes. For CD95L, this was followed by 35 cycles consisting of a 1-minute denaturation at 94°C, 1-minute annealing at 62°C, and a 1-minute extension at 72°C. Reactions were carried out using a Stratagene Mx3000P QPCR System (Stratagene, La Jolla, CA). Ten microliters of PCR product was then size-fractionated on a 2% agarose gel containing ethidium bromide (Sigma-Aldrich, Inc) and photographed under ultraviolet light.

Adenoviral Vector Construction and Infection

The adenoviral (Ad)-CD95L and Ad-CD95L-GFP constructs have previously been described [23]. For the construction of Ad-CD95-GFP, full-length human CD95 cDNA was generated as described above. GFP was attached to the carboxy-terminus of CD95 by cloning the PCR product into the pcDNA3.1/CT-GFP-TOPO vector according to the manufacturer's instructions (Invitrogen). After selection of positive clones, appropriate orientation of the insert was verified by the DNA Sequencing Core Facility at the University of Pittsburgh using the T7 and GFP Reverse primers supplied by Invitrogen. E1- and E3-deleted Ad-CD95-GFP was constructed through Cre-lox recombination as previously described [24]. Briefly, the *CD95-GFP* construct was inserted into the shuttle vector pAdlox, and Ad-CD95-GFP was generated by cotransfection of *Sfi* I–digested pAdlox-CD95-GFP and Ψ5 helper virus DNA into the Ad– packaging cell line CRE8. Recombinant adenoviruses were propagated on CRE8 or 293 cells and purified by cesium chloride density gradient centrifugation and subsequent dialysis. Titers of viral particles were determined by optical densitometry, and 100 particles were estimated to represent 1 PFU. Optimal multiplicity of infection (MOI) was determined using Ad-eGFP and measuring the percentage fluorescent cells 24 and 48 hours later. Approximately 90% transduction was achieved with MOI 100 in Seg-1

and Flo-1 and MOI 50 in MDA468. For all experiments, cells were infected for 6 hours at 37°C in 5% CO_2 using an MOI of 50.

Immunoblot Analysis and Immunoprecipitation

For immunoblot analysis, protein was extracted from subconfluent cultures using lysis buffer (Cell Signaling Technology, Inc) containing 1 mM phenylmethlsulfonylfluoride (Sigma-Aldrich, Inc) and quantified using the BCA protein assay kit (Pierce, Rockford, IL). For immunoprecipitation, cells were first infected with either empty adenovirus (Ad-Ψ5), Ad-CD95-GFP, or Ad-CD95L-GFP as described above. Antibodies were conjugated to Protein-G beads according to the Sigma Protein-G Immunoprecipitation Kit manufacturer's instructions (Sigma-Aldrich, Inc), cell lysate was added to the antibody-conjugated beads, and the mixture was tumbled end-over-end at 4°C for 3 hours. The immunoprecipitate was then centrifuged three times at 16,000*g*, washed with PBS, mixed with sample buffer, and boiled for 5 minutes in preparation for immunoblot analysis. Proteins were resolved using sodium dodecyl sulfate–polyacrylamide gels and subsequently transferred to nitrocellulose membranes (Bio-Rad, Hercules, CA). Membranes were blocked in 5% milk solution, incubated with primary antibody, washed, and incubated with horseradish peroxidase–conjugated secondary antibody. Immunoreactivity was detected using SuperSignal West Pico Chemiluminescent Substrate (Pierce) and x-ray film (Eastman Kodak, Rochester, NY). Blots were stripped with 2% sodium dodecyl sulfate, 100 mM β-mercaptoethanol, and 62.5 mM (pH 6.8) Tris (Sigma-Aldrich, Inc) for 20 minutes at 53°C and reprobed with control antibody.

FACScan Analysis of CD95L Expression and Apoptosis

For analysis of CD95L cell surface expression, subconfluent cultures were incubated for 24 hours in the presence or absence of the broad-spectrum MMP inhibitor GM-6001 (100 μM), harvested with PBS/10 mM EDTA (Sigma-Aldrich, Inc), resuspended in PBS/0.5% normal rabbit serum (Sigma-Aldrich, Inc), and blocked on ice for 15 minutes. Cells were subsequently labeled with anti-CD95L clone NOK-1 antibody and FITC-conjugated secondary antibody (1:200) for 30 minutes each and maintained on ice until analysis. For apoptosis studies, subconfluent cultures were either treated with anti-CD95 activating antibody clone CH11 (20 ng/ml) or infected with Ad-Ψ5 or Ad-CD95L in the presence or absence of the pan-caspase inhibitor zVad (50 μM). Cells were then harvested as described above and stained using the annexin V–FITC apoptosis detection kit (BD Biosciences, San Diego, CA) per the manufacturer's instructions. CD95L expression and apoptosis were assessed by flow cytometry using a Becton Dickinson FACSort (San Jose, CA), and data were analyzed using WinMDI software (Scripps Research Institute, La Jolla, CA).

CD95L ELISA and Isolation of Vesicles

For CD95L ELISA, cells were seeded at 4×10^5 per dish and allowed to proliferate for 5 days (without a medium change). Medium was then collected, and debris were pelleted by centrifugation at 1000*g* for 5 minutes. The supernatant (media) was concentrated 50-fold using Centricon YM-10 filters (Fisher Scientific, Pittsburgh, PA), and soluble CD95L (sCD95L) expression was analyzed by commercially available ELISA (R&D Systems, Minneapolis, MN) according to the manufacturer's instructions. For isolation of vesicles, supernatant (media) was recovered from subconfluent cultures and was subjected to three successive centrifugations at 300*g* (5 minutes), 1200*g* (20 minutes), and 10,000*g* (30 minutes) to eliminate cells and debris, followed by centrifugation for 1 hour at 100,000*g*. To remove excess serum proteins, the vesicle pellet was washed with a large volume of PBS, centrifuged at 100,000*g* for 1 hour, and finally resuspended in 100 μl of PBS. Protein was then quantified and examined by immunoblot analysis as described above.

Laser Scanning Confocal Microscopy

Cells were plated on glass coverslips and allowed to reach 50% confluence. For CD95L microscopy, cells were then fixed with 2% paraformaldehyde, permeabilized with 1% Triton-X, and blocked for 45 minutes in a 1:20 dilution of normal goat serum (Sigma-Aldrich, Inc) in PBS. After several washes with 0.1% BSA (Sigma-Aldrich, Inc), the coverslips were maintained on ice and labeled with either anti-CD95L clone G247-4 (1:100) or anti-CD95 clone CH11 (1:100) followed by Cy3-conjugated secondary antibody (1:1000) for 1 hour each. Nuclei were stained with Draq5 for 5 minutes (1:1000), and coverslips were mounted with gelvatol and stored overnight at 4°C. For dual (CD95/CD95L) staining, 50% confluent cells were first infected with either Ad-CD95-GFP or Ad-CD95L-GFP and then stained as described above. Cells were viewed the following day using an Olympus FluoView 1000 confocal microscope (Olympus, Inc, Center Valley, PA).

Results

CD95L Is Expressed in a Variety of Human Cell Lines

CD95L expression has previously been demonstrated in surgical specimens of esophageal and other adenocarcinomas [25], but the expression of CD95L in adenocarcinoma cell lines has not been well characterized. CD95L mRNA was detected in all five human cell lines including immortalized HET-1A and BAR-T cells (Figure 1*A*). By immunoblot, both the membranous (34 kDa) and soluble (21 kDa) forms of CD95L were detected in the positive control KFL cells, whereas in most experiments, only sCD95L was observed in the other cell lines (Figure 1*B*). Comparatively small quantities of mCD95L were occasionally observed in Flo-1 and Seg-1 cells. CD95L protein expression was greatest in the positive control KFL and adenocarcinoma Seg-1 cell lines, with slightly lower levels of CD95L protein observed in Bic-1 cells. The CD95L protein level detected in Flo-1 cells was similar to that observed in the immortalized Het-1A and BAR-T cell lines. Taken together, our *in vitro* observations are consistent with the previously reported *in situ* expression of CD95L in esophageal, colon, and lung adenocarcinomas [25–27], validating these cell lines as models consistent with surgical specimens.

CD95L Is Not Trafficked to the Cell Membrane

Increased expression of CD95L is putatively advantageous to tumors through down-regulation of the immune response through induction of apoptosis in tumor-infiltrating lymphocytes (TILs), a concept coined the "counterattack hypothesis" [13]. Because we observed the soluble form (sCD95L) expressed by the adenocarcinoma cell lines, we hypothesized that CD95L is trafficked to the cell membrane and secreted. To the contrary, we were unable to demonstrate cell surface expression of CD95L, even after MMP inhibition in any

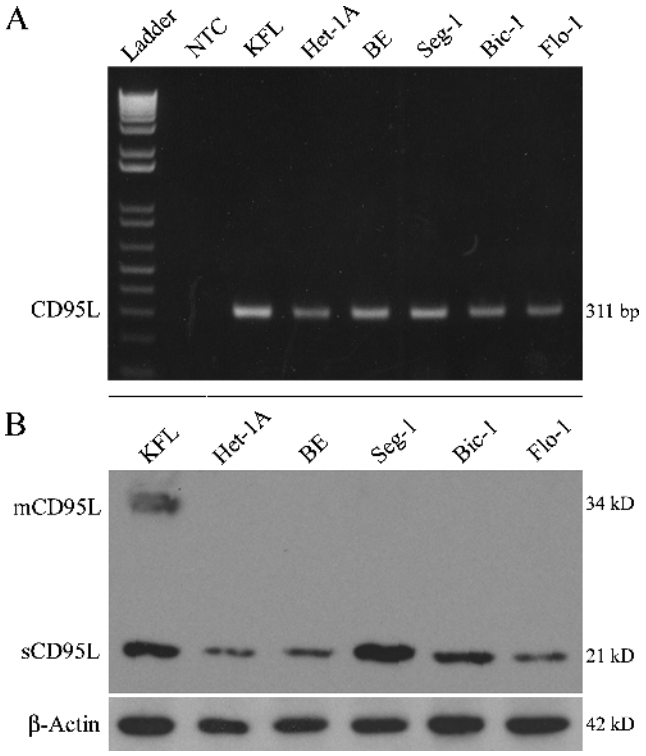

Figure 1. CD95L expression in a panel of human cell lines. (A) Reverse transcription–polymerase chain reaction analysis of CD95L mRNA expression. (B) Immunoblot analysis of CD95L protein expression using the G247-4 antibody. mCD95L was detected only in KFL cells, whereas sCD95L was expressed by all cell lines examined. Results are representative of at least three individual experiments. NTC indicates no template control.

of the cell lines (Figure 2*A*). Furthermore, ELISA did not identify the presence of secreted CD95L in the culture medium (Figure 2*B*).

Regulation of CD95L expression is complex and is determined not only by transcriptional and translational activity but also through posttranslational processing [28,29]. Secretion of CD95L in membrane-bound vesicles by neoplasms has been described [30]. Thus, we investigated the hypothesis that the observed CD95L was being packaged into vesicles for secretion. Vesicle production was observed in the EA cell line Flo-1 and, to a far lesser extent, in Seg-1 adenocarcinoma cell line based on protein quantification of the isolated vesicles (data not shown), yet CD95L was not detectable in the isolated vesicles (Figure 2*C*). Furthermore, laser scanning confocal microscopy demonstrated cytoplasmic expression of CD95L in the Flo-1 cell line (Figure 2*D*). Taken together, these observations suggest that adenocarcinoma cells sequester cleaved, sCD95L in the cytoplasm and do not traffic the protein to the cell membrane or secrete it through vesicles.

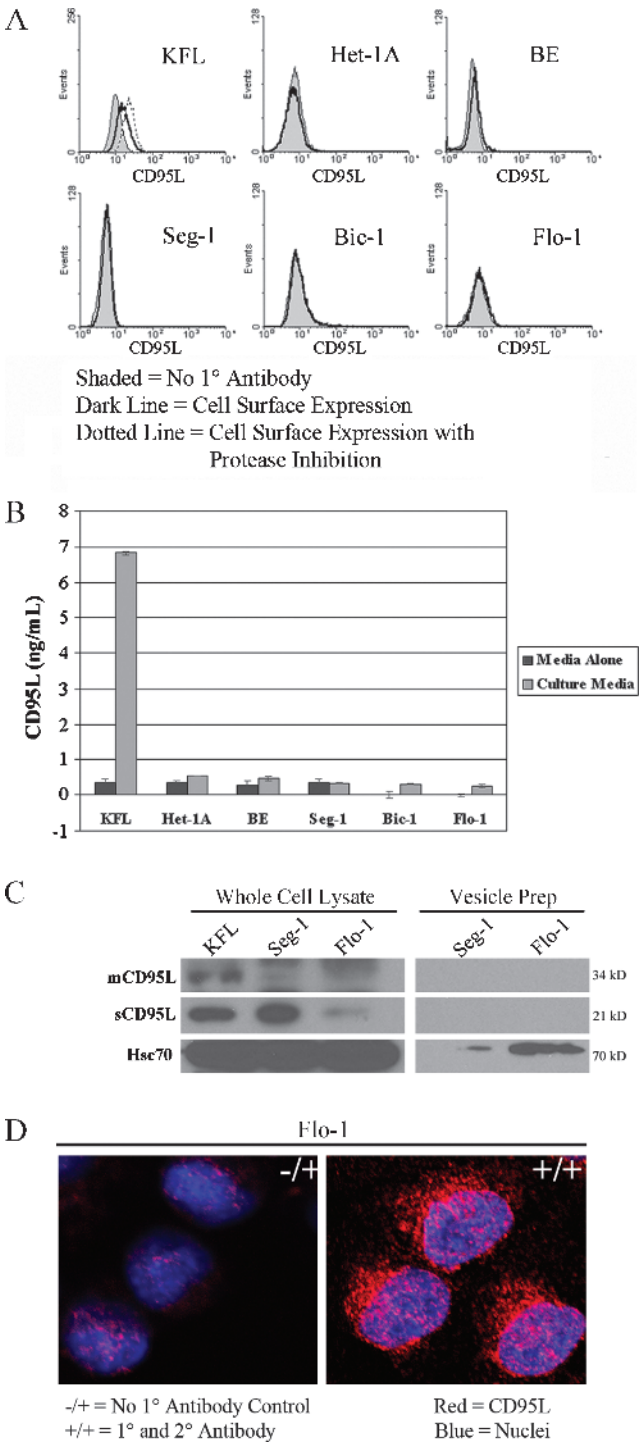

Figure 2. Subcellular localization of CD95L. (A) FACScan analysis of CD95L cell surface expression (shaded histograms represent no primary antibody controls; open histograms represent experimental groups in the absence [solid lines] or presence [dashed lines] of MMP inhibition). Cell surface expression of CD95L was not detected in any of the esophageal or adenocarcinoma cell lines, even after MMP inhibition. (B) CD95L ELISA of culture medium. Data are presented as mean concentration (ng/ml) ± SEM of three individual experiments. Secretion of CD95L by the esophageal and adenocarcinoma cell lines was negligible or absent. (C) Immunoblot of CD95L expression in whole cell lysates and vesicle preparations from the adenocarcinoma cell lines Seg-1 and Flo-1. Vesicles were detected and isolated from Flo-1 cells and to a lesser degree from Seg-1 cells (as evidenced by Hsc70 immunoreactivity [36]), but CD95L was not detected by immunoblot analysis these vesicle preparations. (D) Laser scanning confocal microscopy of CD95L in the EA cell line Flo-1 (magnification, ×400). CD95L is predominantly localized to the cytoplasm in a perinuclear distribution. −/+ indicates represents no primary antibody control; blue, nuclei; red, CD95L. All results are representative of at least three individual experiments.

Intracellular CD95-CD95L Interactions

Combined with our previously reported cytoplasmic retention of CD95 in Flo-1 cells [19], these current observations led us to hypothesize that intracellular CD95-CD95L interactions may be occurring. For these studies, we used a fusion protein strategy whereby either CD95 or CD95L was conjugated to GFP and delivered using E1 and E3 deleted adenoviral infection. Similar to the expression of native CD95 and CD95L in these cells, both the Ad-CD95-GFP and Ad-CD95L-GFP constructs resulted in predominantly cytoplasmic expression of CD95 and CD95L; furthermore, a moderate degree of colocalization was apparent (Figure 3*A*). However, we were unable to demonstrate an interaction by immunoprecipitation of GFP after infection with Ad-CD95-GFP (Figure 3*B*) or Ad-CD95L-GFP (data not shown). Thus, whereas there is a degree of colocalization, we were unable to demonstrate an intracellular CD95-CD95L protein interaction.

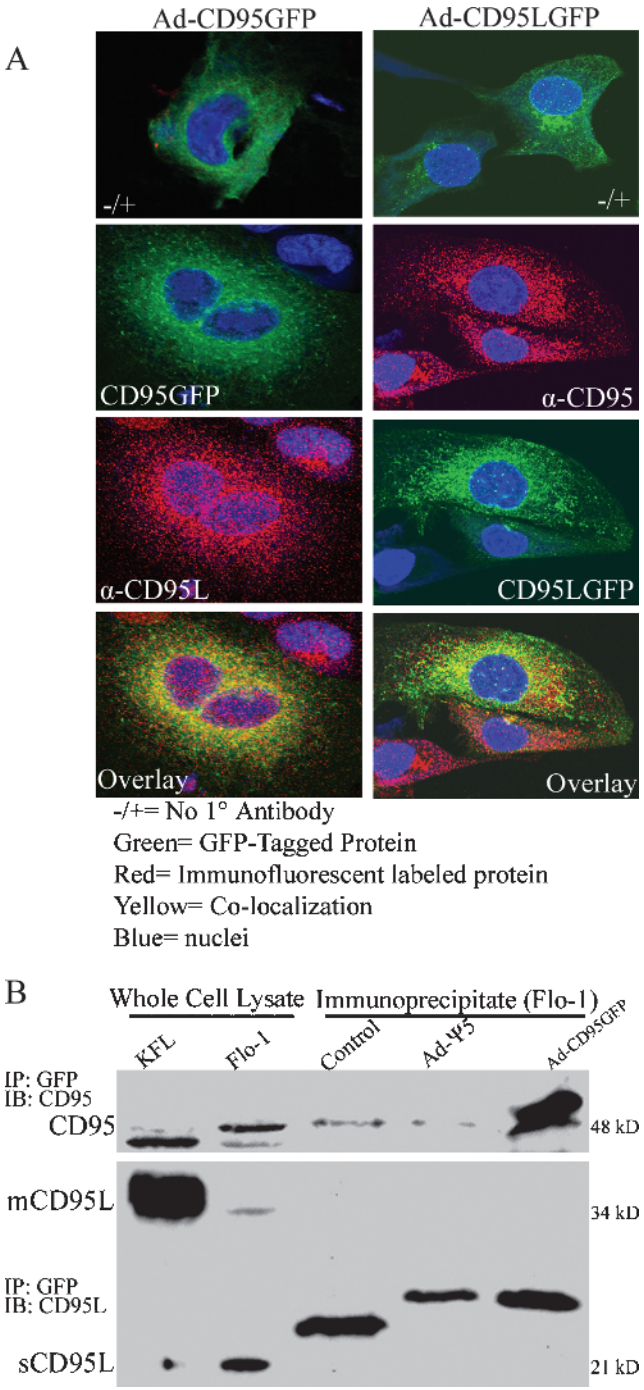

Figure 3. Intracellular interaction of CD95 and CD95L. (A) Laser scanning confocal microscopy of CD95 and CD95L in Flo-1 cells after infection with either Ad-CD95-GFP (left column) or Ad-CD95L-GFP (right column) as described in Materials and Methods (magnification, ×400). In the left column, CD95 appears green and CD95L appears red, whereas CD95 appears red and CD95L appears green in the right column. Similar to the expression of the native proteins, both Ad-CD95-GFP and Ad-CD95L-GFP predominantly localize in the cytoplasm. A modest degree of CD95-CD95L colocalization was apparent after infection with both adenoviral constructs. (B) Immunoblot of CD95 and CD95L in Flo-1 cells after infection with Ad-CD95-GFP and immunoprecipitation of GFP. GFP immunoprecipitation was confirmed by detection of CD95 at an expected, slightly larger molecular weight, but neither mCD95L nor sCD95L was coprecipitated. Nonspecific immunoprecipitate bands in the CD95L immunoblot represent BSA antibody light chain (Control) and GFP antibody light chain (Ad-Ψ5 and Ad-CD95-GFP). Results are representative of three individual experiments.

Expression of Cytoplasmic CD95L Overcomes Resistance to CD95-Mediated Apoptosis

Given the altered expression and potential cytoplasmic interaction of CD95 and CD95L in Flo-1 cells, we hypothesized that stimulation of the intracellular pool of CD95 would result in alternative signaling. JTCs, which abundantly express CD95 on the cell membrane [31], are sensitive to extracellular CD95 stimulation and served as a positive control. CD95-null MDA468 cells served as a negative control [32]. Treatment with activating anti-CD95 antibody (CH11) induced apoptosis only in JTC and, to a lesser extent, in Seg-1 cells. Surprisingly, overexpression of cytoplasmic CD95L (after treatment with Ad-CD95L) induced robust apoptosis in Seg-1 and Flo-1 cells leading to complete loss of the cultures, and this response was inhibited by zVad (Figure 4, *A* and *B*). Neither activating anti-CD95 antibody nor Ad-CD95L resulted in apoptosis in CD95-null MDA468 cells. Apoptosis was further confirmed by immunoblot analysis for cleaved caspase 8 and caspase 3 in the EA cell line Flo-1 (Figure 4*C*). Importantly, these findings show that overexpression of cytoplasmic CD95L induces extensive apoptosis in otherwise CD95-resistant adenocarcinoma cells.

Several reports have demonstrated that CD95 signaling may also result in activation of nonapoptotic signaling pathways [5–8]. Because pan-caspase inhibition with zVad inhibited Ad-CD95L–induced apoptosis, we hypothesized that CD95-CD95L interactions under these circumstances would result in nonapoptotic signaling. Extracellular-regulated kinase (ERK) was phosphorylated in untreated Flo-1 cells, and none of the treatments alone (activating anti-CD95 antibody, control virus, or Ad-CD95L) resulted in significant ERK phosphorylation. In the presence of pan-caspase inhibition, however, treatment with Ad-CD95L induced robust phosphorylation of ERK (Figure 4*D*). We attempted to further confirm that CD95-CD95L interactions contribute to constitutive MAP-k signaling by determining the effects of silencing CD95L mRNA expression but failed because of small interfering RNA transfection efficiency and other challenges. Thus, in the setting of downstream (pan-caspase) inhibition of apoptosis pathways and overexpression of CD95L, cytoplasmic CD95-CD95L

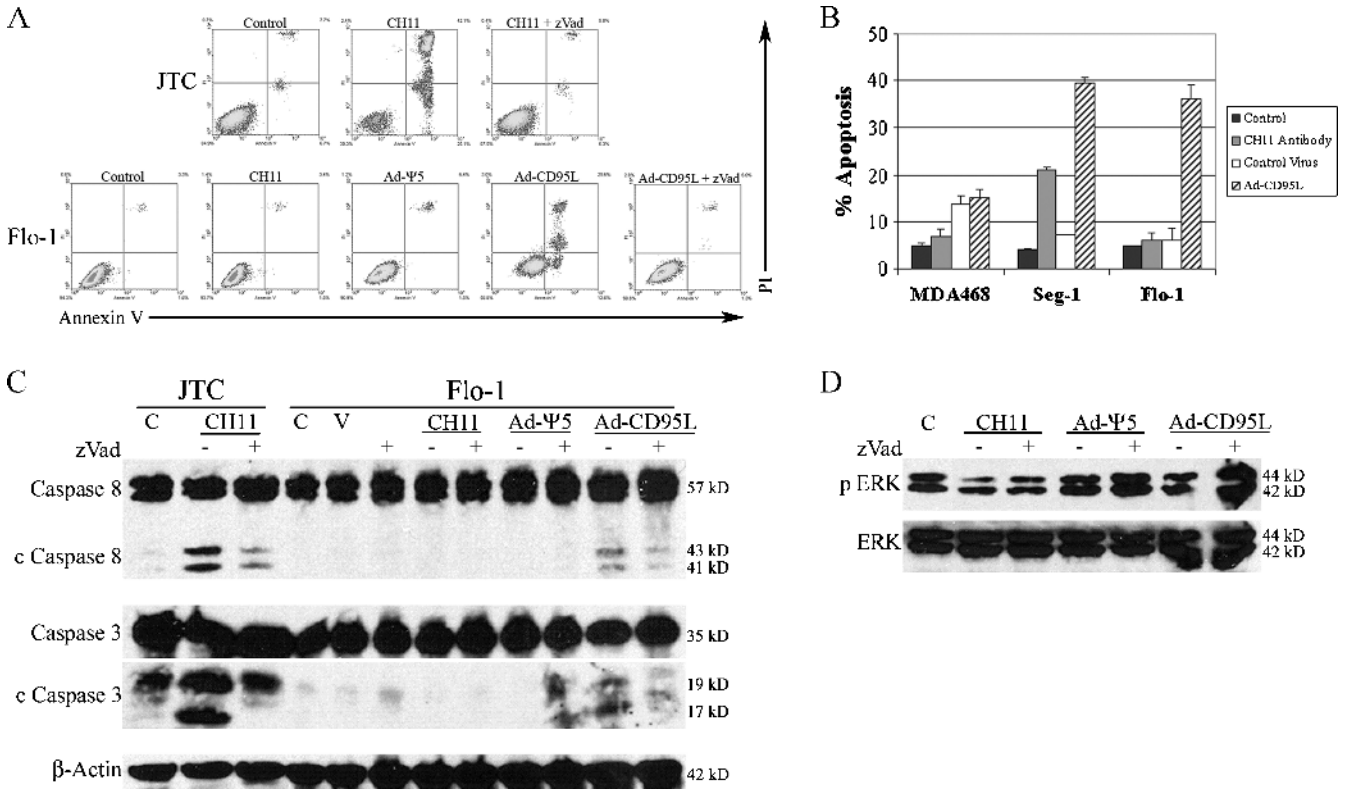

Figure 4. Effects of extracellular compared with intracellular stimulation of CD95. (A) FACScan analysis of annexin V (AV)– and propidium iodide (PI)–stained JTC and Flo-1 cells 24 hours after treatment with activating CD95 antibody (CH11), control virus (Ad-Ψ5), or Ad-CD95L in the presence or absence of the pan-caspase inhibitor zVad. Positive staining for AV suggests early apoptosis (right lower quadrant). Positive staining for PI suggests loss of membrane integrity late in apoptosis (right upper quadrant) or due to necrosis (left upper quadrant). CH11 induced massive cell death in CD95-sensitive JTC but had no effect in Flo-1 cells, whereas Ad-CD95L induced cell death in Flo-1. Addition of zVad inhibited cell death induced by both CH11 (JTC) and Ad-CD95L (Flo-1), suggesting that these treatments induce apoptosis. (B) Bar graph depicting percent apoptosis in CD95-null MDA468 cells and the adenocarcinoma cell lines Seg-1 and Flo-1 after treatments as described above. Data are presented as mean percent apoptosis (sum of % AV-positive and % AV/PI-positive cells) ± SEM of three individual experiments. Neither CH11 nor Ad-CD95L induced apoptosis (compared with controls) in MDA468 cells. CH11 induced apoptosis in Seg-1 but not Flo-1 cells, whereas Ad-CD95L resulted in apoptosis in both adenocarcinoma cell lines. (C) Immunoblots of caspase 8 and caspase 3 in JTC and Flo-1 cells after treatments as described above. CH11 induced caspase 8 and caspase 3 cleavage in JTC but not Flo-1 cells, whereas Ad-CD95L induced cleavage of both caspase 8 and caspase 3 in Flo-1 cells. Caspase cleavage was attenuated by zVad after both treatments. C indicates control; V, vehicle (DMSO). (D) Immunoblots of phosphorylated ERK (p ERK) and total ERK in Flo-1 cells after treatments as described above. ERK was phosphorylated in control (C) cells, and infection with Ad-CD95L (in the presence of zVad) induced further phosphorylation of ERK.

interactions result in activation of nonapoptotic signaling pathways, but a role for low-level CD95-CD95L interactions contributing to constitutive MAP-k signaling could not be confirmed.

Discussion

We have shown that CD95L is expressed at both the RNA and protein levels in a panel of cell lines derived from EA and other human tissues. Size-fractionation suggests the protein is predominantly cleaved to sCD95L; mCD95L was relatively absent by immunoblot or FACScan analysis or laser scanning confocal microscopy. CD95L was neither trafficked to the cell membrane nor secreted into the medium or within vesicles, rather the protein seems to be sequestered in the cytoplasm. CD95 and CD95L colocalize by immunofluorescence, but an interaction could not be demonstrated by immunoprecipitation. Overexpression of CD95L in the EA cell line Flo-1 induced robust apoptosis and under conditions of pan-caspase inhibition, resulted in activation of ERK signaling. Taken together, our findings imply that CD95L expression by neoplasms may confer prosurvival and proliferation functions; however, these end points were not specifically shown. Furthermore, the robust induction of apoptosis after overexpression of CD95L, confined to the cytoplasm, suggests that the posttranslational regulation of cell surface levels of death receptors is an important mechanism of resistance to extracellular apoptotic signals.

These findings are inconsistent with previous reports suggesting an immune privilege function of CD95L expression in esophageal cancer through induction of apoptosis in TILs [25,33]. We were unable to demonstrate cell surface expression of CD95L in any of our cell lines, even after treatment with a MMP inhibitor (Figure 2*A*). Reports have supported a role for modulation of tumoral immunity in melanoma and head and neck cancer where secretion of CD95L in membrane-bound vesicles has been suggested to result in modulation of the immune system in tumor-bearing host [30]. CD95L protein

was not present in isolated secretory vesicles from Seg-1 and Flo-1 cells (Figure 2*C*). Thus, our findings are not consistent with CD95L expression in EA contributing to direct effects on TILs or the circulating cytokine mileu. Finally, given a recent report showing mCD95L is essential for CD95-induced apoptosis [18], our observation of sCD95L protein and the lack of mCD95L indirectly supports the notion of a nonapoptotic function of CD95L expression in adenocarcinoma.

Our previously reported observation of cytoplasmic retention of CD95 in these same cell lines [19] led us to postulate that CD95L expression and intracellular CD95-CD95L interactions contributed to this phenotype. Because of reagent limitations that affect dual labeling and immunoprecipitation of the native proteins, we used a GFP fusion protein strategy. We were unable to demonstrate an interaction by immunoprecipitation, but this may represent a technical problem or a low-affinity protein-protein interaction, as laser scanning confocal microscopy suggested a modest degree of colocalization (Figure 3). Furthermore, Ad-CD95L induced robust apoptosis within 6 hours of infection in all cell lines except for CD95-null MDA468 cells (Figure 4*B*). This finding supports the hypothesis that CD95L is capable of interacting with the cytoplasmic pool of CD95 and demonstrating that the apoptotic machinery downstream of CD95 is intact. This has important implications regarding regulation of cell sensitivity to extracellular signaling for apoptosis. This finding demonstrates that decreased cell surface expression alone is sufficient to render cells resistant to CD95-mediated apoptosis, and this mechanism may have been underappreciated in other studies that focus on downstream modulation of apoptotic pathways.

Our observation of increased ERK1/2 phosphorylation after Ad-CD95L infection supports the notion that CD95L expression may confer functions beneficial to neoplasia and is consistent with the findings of others [5–8]. CD95 signaling has been shown to be important for hepatocyte regeneration after hepatectomy [34] and neurite outgrowth after injury [35]. Furthermore, there are reports of activation of NF-κB, p38, and ERK1/2 in various tumor cell lines leading to proliferation and tumor progression [5–7]. In Flo-1 EA cells, ERK1/2 was constitutively phosphorylated, and this was further enhanced after CD95 activation with Ad-CD95L but only under conditions of pan-caspase inhibition (Figure 4*D*). Thus, our data are consistent with growing evidence of nonapoptotic functions for CD95 under conditions of dysfunctional downstream apoptotic signaling that may confer advantages to tumor cells and help explain the observed absence of mutations or loss of expression of CD95 in neoplasia.

In summary, we have documented CD95L expression in a panel of human esophageal and various adenocarcinoma cell lines. Similar to CD95 expression in these cell lines, CD95L was sequestered in the cytoplasm. Stimulation of the intracellular pool of CD95 induced robust apoptosis in otherwise CD95-resistant Flo-1 cells and resulted in ERK activation under conditions of pan-caspase inhibition. Thus, posttranslational regulation of cell surface expression of death receptors is an important modulator of cell sensitivity to external signals for apoptosis. Our data support the potential for therapies aimed at increasing cytoplasmic CD95L expression in CD95-resistant cells and support the concept that, under certain conditions, CD95 stimulation may result in activation of nonapoptotic signaling pathways.

References

[1] Ehrenschwender M and Wajant H (2009). The role of FasL and Fas in health and disease. *Adv Exp Med Biol* **647**, 64–93.

[2] Guicciardi ME and Gores GJ (2009). Life and death by death receptors. *FASEB J* **23**, 1625–1637.

[3] Lee KH, Feig C, Tchikov V, Schickel R, Hallas C, Schutze S, Peter ME, and Chan AC (2006). The role of receptor internalization in CD95 signaling. *EMBO J* **25**, 1009–1023.

[4] Owen-Schaub L, Chan H, Cusack JC, Roth J, and Hill LL (2000). Fas and Fas ligand interactions in malignant disease. *Int J Oncol* **17**, 5–12.

[5] O'Brien DI, Nally K, Kelly RG, O'Connor TM, Shanahan F, and O'Connell J (2005). Targeting the Fas/Fas ligand pathway in cancer. *Expert Opin Ther Targets* **9**, 1031–1044.

[6] Peter ME, Budd RC, Desbarats J, Hedrick SM, Hueber AO, Newell MK, Owen LB, Pope RM, Tschopp J, Wajant H, et al. (2007). The CD95 receptor: apoptosis revisited. *Cell* **129**, 447–450.

[7] Wajant H, Pfizenmaier K, and Scheurich P (2003). Non-apoptotic Fas signaling. *Cytokine Growth Factor Rev* **14**, 53–66.

[8] Chen L, Park SM, Tumanov AV, Hau A, Sawada K, Feig C, Turner JR, Fu YX, Romero IL, Lengyel E, et al. (2010). CD95 promotes tumour growth. *Nature* **465**, 492–496.

[9] Ferguson TA and Griffith TS (2006). A vision of cell death: Fas ligand and immune privilege 10 years later. *Immunol Rev* **213**, 228–238.

[10] Filippini A, Riccioli A, Padula F, Lauretti P, D'Alessio A, De Cesaris P, Gandini L, Lenzi A, and Ziparo E (2001). Control and impairment of immune privilege in the testis and in semen. *Hum Reprod Update* **7**, 444–449.

[11] Guller S and LaChapelle L (1999). The role of placental Fas ligand in maintaining immune privilege at maternal-fetal interfaces. *Semin Reprod Endocrinol* **17**, 39–44.

[12] Hahne M, Rimoldi D, Schroter M, Romero P, Schreier M, French LE, Schneider P, Bornand T, Fontana A, Lienard D, et al. (1996). Melanoma cell expression of Fas(Apo-1/CD95) ligand: implications for tumor immune escape. *Science* **274**, 1363–1366.

[13] O'Connell J, O'Sullivan GC, Collins JK, and Shanahan F (1996). The Fas counterattack: Fas-mediated T cell killing by colon cancer cells expressing Fas ligand. *J Exp Med* **184**, 1075–1082.

[14] Whiteside TL (2007). The role of death receptor ligands in shaping tumor microenvironment. *Immunol Invest* **36**, 25–46.

[15] Kozlowski M, Kowalczuk O, Sulewska A, Dziegielewski P, Lapuc G, Laudanski W, Niklinska W, Chyczewski L, Niklinski J, and Laudanski J (2007). Serum soluble Fas ligand (sFasL) in patients with primary squamous cell carcinoma of the esophagus. *Folia Histochem Cytobiol* **45**, 199–204.

[16] Houston AM, Michael-Robinson JM, Walsh MD, Cummings MC, Ryan AE, Lincoln D, Pandeya N, Jass JR, Radford-Smith GL, and O'Connell J (2008). The "Fas counterattack" is not an active mode of tumor immune evasion in colorectal cancer with high-level microsatellite instability. *Hum Pathol* **39**, 243–250.

[17] Ryan AE, Shanahan F, O'Connell J, and Houston AM (2005). Addressing the "Fas counterattack" controversy: blocking fas ligand expression suppresses tumor immune evasion of colon cancer *in vivo*. *Cancer Res* **65**, 9817–9823.

[18] O'Reilly LA, Tai L, Lee L, Kruse EA, Grabow S, Fairlie WD, Haynes NM, Tarlinton DM, Zhang JG, Belz GT, et al. (2009). Membrane-bound Fas ligand only is essential for Fas-induced apoptosis. *Nature* **461**, 659–663.

[19] Hughes SJ, Nambu Y, Soldes OS, Hamstra D, Rehemtulla A, Iannettoni MD, Orringer MB, and Beer DG (1997). Fas/APO-1 (CD95) is not translocated to the cell membrane in esophageal adenocarcinoma. *Cancer Res* **57**, 5571–5578.

[20] Nambu Y, Hughes SJ, Rehemtulla A, Hamstra D, Orringer MB, and Beer DG (1998). Lack of cell surface Fas/APO-1 expression in pulmonary adenocarcinomas. *J Clin Invest* **101**, 1102–1110.

[21] Haefner B (2006). Targeting NF-κB in anticancer adjunctive chemotherapy. *Cancer Treat Res* **130**, 219–245.

[22] Jaiswal KR, Morales CP, Feagins LA, Gandia KG, Zhang X, Zhang HY, Hormi-Carver K, Shen Y, Elder F, Ramirez RD, et al. (2007). Characterization of telomerase-immortalized, non-neoplastic, human Barrett's cell line (BAR-T). *Dis Esophagus* **20**, 256–264.

[23] Mohammad RM, Banerjee S, Li Y, Aboukameel A, Kucuk O, and Sarkar FH (2006). Cisplatin-induced antitumor activity is potentiated by the soy isoflavone genistein in BxPC-3 pancreatic tumor xenografts. *Cancer* **106**, 1260–1268.

[24] Sandur SK, Ichikawa H, Sethi G, Ahn KS, and Aggarwal BB (2006). Plumbagin (5-hydroxy-2-methyl-1,4-naphthoquinone) suppresses NF-κB activation and NF-κB–regulated gene products through modulation of p65 and IκBα kinase activation, leading to potentiation of apoptosis induced by cytokine and chemotherapeutic agents. *J Biol Chem* **281**, 17023–17033.

[25] Kase S, Osaki M, Adachi H, Kaibara N, and Ito H (2002). Expression of Fas and Fas ligand in esophageal tissue mucosa and carcinomas. *Int J Oncol* **20**, 291–297.

[26] Ding EX, Hizuta A, Morimoto Y, Tanida T, Hongo T, Ishii T, Yamano T, Fujiwara T, Iwagaki H, and Tanaka N (1998). Human colon cancer cells express the functional Fas ligand. *Res Commun Mol Pathol Pharmacol* **101**, 13–24.

[27] Niehans GA, Brunner T, Frizelle SP, Liston JC, Salerno CT, Knapp DJ, Green DR, and Kratzke RA (1997). Human lung carcinomas express Fas ligand. *Cancer Res* **57**, 1007–1012.

[28] Curtin JF and Cotter TG (2003). Live and let die: regulatory mechanisms in Fas-mediated apoptosis. *Cell Signal* **15**, 983–992.

[29] Kavurma MM and Khachigian LM (2003). Signaling and transcriptional control of Fas ligand gene expression. *Cell Death Differ* **10**, 36–44.

[30] Bergmann C, Strauss L, Wieckowski E, Czystowska M, Albers A, Wang Y, Zeidler R, Lang S, and Whiteside TL (2009). Tumor-derived microvesicles in sera of patients with head and neck cancer and their role in tumor progression. *Head Neck* **31**, 371–380.

[31] Peter ME, Dhein J, Ehret A, Hellbardt S, Walczak H, Moldenhauer G, and Krammer PH (1995). APO-1 (CD95)–dependent and –independent antigen receptor–induced apoptosis in human T and B cell lines. *Int Immunol* **7**, 1873–1877.

[32] Stang MT, Armstrong MJ, Watson GA, Sung KY, Liu Y, Ren B, and Yim JH (2007). Interferon regulatory factor-1–induced apoptosis mediated by a ligand-independent fas-associated death domain pathway in breast cancer cells. *Oncogene* **26**, 6420–6430.

[33] Bennett MW, O'Connell J, O'Sullivan GC, Brady C, Roche D, Collins JK, and Shanahan F (1998). The Fas counterattack *in vivo*: apoptotic depletion of tumor-infiltrating lymphocytes associated with Fas ligand expression by human esophageal carcinoma. *J Immunol* **160**, 5669–5675.

[34] Desbarats J and Newell MK (2000). Fas engagement accelerates liver regeneration after partial hepatectomy. *Nat Med* **6**, 920–923.

[35] Desbarats J, Birge RB, Mimouni-Rongy M, Weinstein DE, Palerme JS, and Newell MK (2003). Fas engagement induces neurite growth through ERK activation and p35 upregulation. *Nat Cell Biol* **5**, 118–125.

[36] Lancaster GI and Febbraio MA (2005). Exosome-dependent trafficking of HSP70: a novel secretory pathway for cellular stress proteins. *J Biol Chem* **280**, 23349–23355.